Transactions on Engineering and Computing Sciences - Vol. 11, No. 2
Publication Date: April 25, 2023
DOI:10.14738/tecs.112.14452.
Toma, S., Seto, K., & Chen, W. F. (2023). Dynamic Analysis for Overturning of Pile Driving Machine, etc., on Soft Ground. Transactions on Engineering and Computing Sciences, 11(2). 61-81.

SERVICES FOR SCIENCE AND EDUCATION

Dynamic Analysis for Overturning of Pile Driving Machine, etc., on Soft Ground

Shouji Toma
Hokkai-Gakuen University, Sapporo, Japan

Kenji Seto
Hokkai-Gakuen University, Sapporo, Japan

Wai Fah Chen
University of Hawaii, Hawaii, USA

ABSTRACT

There were quite a few overturning accidents of heavy machinery which have a high center of gravity such as pile driving machines, cranes, jacks, or working vehicles with aerial platform. Researches to study the background of the accidents have taken place from the structural stability point of view by the authors. The structural instability, as can be seen typically in the elastic buckling of columns, may be a blind spot because the structures deflect in different directions to that of the load, which makes it difficult to predict. According to the past investigations, the overturning mechanisms can be categorized into the three: (1) Type of overturning moment, (2) Type of structural instability and (3) Type of equilibrium transition, in which Type of equilibrium transition plays important role on the overturning on soft ground. The past investigations were based on the static analysis. Dynamic analysis is essential to include the effect of inertial forces which will significantly affect the overturning accidents on the soft ground. In the static analysis, the displacement inclination is considered to stop at the equilibrium position, but in the dynamic analysis it will continue increasing due to the inertial force. Then, it is possible the displacement may go beyond the equilibrium and even the stability limit to overturn. In this paper, the equations of motion will be first introduced, then behaviors of the machinery from time to time, i.e., the inclination-time curves, will be obtained by solving the equations. It is shown that the dynamic analysis can explain more precisely the overturning behaviors of the machinery on the soft foundation than the static analysis.

Keywords: Overturning Accident, Overturning Mechanism, Pile Driving Machine, Crane, Structural Stability, Soft Foundation, Initial Imperfections

INTRODUCTION

Overturning accidents of cranes, pile driving machines, Jacks, working vehicles with aerial platform, etc., on soft ground have occurred frequently in Japan [1 ~ 3]. In the United States, the Pile Driving Contractors Association (PDCA) also has a great concern on the accidents by providing the information for the safe working platforms at the construction site [4, 5]. In

general, the investigation of the causes is focused on comparing the ground strength to the working pressure induced by the overturning moment [6]. On the other hand, in the early studies it is pointed out that the theory of structural stability which can be seen typically in the column buckling should be considered to investigate the causes of the overturning accidents, and that a high center of gravity which may lead to the structural instability exists commonly as the background of these accidents [7 ~ 9]. In the past, the fall accidents of bridge girders by the overturning jacks were first studied [10], then the overturning behaviors of heavy machinery such as pile driving machines or cranes which have a high center of gravity were investigated [11, 12]. They are published in the international engineering journals as well [13, 14].

However, those researches are based only on the static analysis and the dynamic effect due to the inertia force is not included. The dynamic analysis is essential to understand the overturning mechanism more in detail. In this paper, the past static analyses are outlined at the beginning, in which the overturning mechanism can be categorized into the three: (1) Type of overturning moment, (2) Type of structural instability and (3) Type of equilibrium transition. It is found that the type of equilibrium transition plays an important role on the overturning on soft ground. Then, the equations of motion are derived for the dynamic analysis and solved to obtain the displacement inclination change against time by oscillation. By the dynamic analysis the mechanism will be explained how the initial inclination amplifies the inclination of the machinery, thus increasing the possibility of the overturning.

This paper aims to understand generally the overturning mechanisms of the heavy machinery from the stability point of view. Therefore, only the transverse direction of overturning is discussed without any other directions and the attenuating force is disregarded.

OVERTURNING MECHANISMS BY STATIC ANALYSIS

Structural Model and Equilibrium Equations

Since details of the relationship of the load and the displacement inclination are described in the previous papers [10 ~ 14], only the outline will be given in this paper. The structural model in the static analysis assumes that, as shown in Fig. 1, the whole machine is rigid with sufficiently large stiffness and connected to the ground with the rotational spring stiffness. Whole weight of the machine is considered to concentrate at the center of gravity which is calculated by applying the first degree of moment.

The equilibrium of moment in Fig. 1 leads to the following equation [15]:

$$Ks(\theta - \theta_o) - P(L\sin\theta + e\cos\theta) = 0 \qquad (1)$$

in which Ks = rotational spring stiffness (assumed as linear), P = load (whole weight of machine), L = height of load, θ= displacement inclination, θ_o= initial inclination, e = eccentricity of load

The first term of Eq. (1) is the righting moment and the second is the overturning moment. It should be noted that *Ks* in Eq. (1) is assumed as linear, therefore the righting moment in Eq. (1) will be increased unlimitedly as θ increases. From Eq. (1) the load-displacement relationship is derived as follows:

$$P = \frac{Ks(\theta - \theta o)}{L\sin\theta + e\cos\theta} \qquad (2)$$

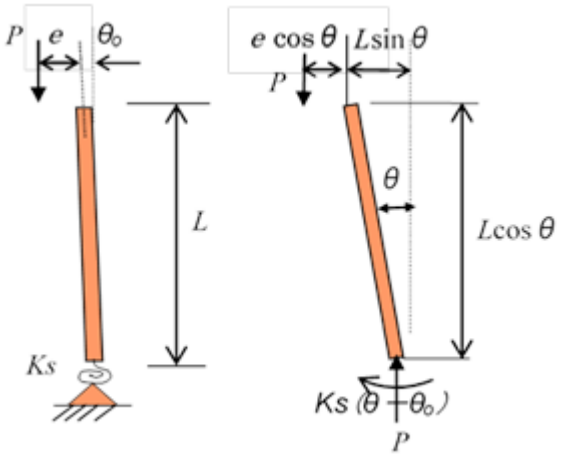


Figure 1. Structural Model in Static Analysis.

Assuming in Eq. (2) that the initial imperfections are zero, i.e., $\theta o = 0$ and $e = 0$, and that the displacement inclination is infinitesimal, the eigenvalue load for overturning P_{cr} will be derived as follows:

$$P_{cr} = Ks / L \qquad (3)$$

The load in Eq. (3) corresponds to the Euler load in the elastic column buckling. Non-dimensioning *P* of Eq. (2) by P_{cr} of Eq. (3) gives

$$\frac{P}{P_{cr}} = \frac{\theta - \theta o}{\sin\theta + e\cos\theta / L} \qquad (4)$$

Using Eq. (4), a relationship between the load and displacement inclination is plotted in Fig. 2. It can be found that the displacement is increased significantly by the effect of the initial inclination.

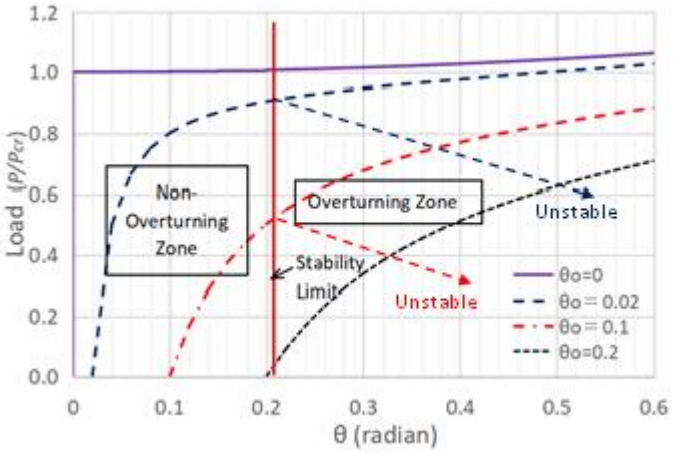


Figure 2. Load-inclination curves with initial inclination (e = 0).

Stability Limit

In Fig. 2, the stability limit θ_u is shown just for reference, which is defined by the Eq. (5).

$$\theta_u = \tan^{-1}\frac{S}{2L} \qquad (5)$$

in which S = width of footing.

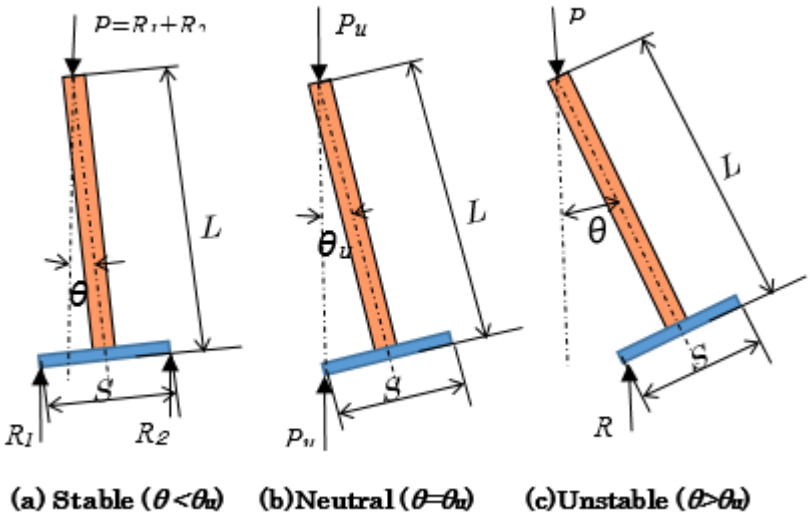


Figure 3. Concept of Stable and Unstable.

Figure 3 is a category of the concept of stable and unstable. The neutral of Fig. 3 (b) is the stability limit, Eq. (5), at which the directions of the load and the support are on the same vertical line. When the displacement inclination is larger than the stability limit, the equilibrium curve becomes descent (unstable) as shown in Fig. 2, for the machine to overturn. Accordingly,

the intersection of the stability limit and the equilibrium curve expresses the overturning load which is reduced significantly by the effect of the initial inclination.

Type of Equilibrium Transition [13]

As stated above, the machine on the soft ground might be overturned by the mechanism "Type of equilibrium transition". Figure 4 describes a sample of the load-displacement curves and illustrates the mechanism. Suppose that at the beginning the machine stays at an equilibrium point A on the curve, then moves to a softer position B' for some unexpected reasons. Then, the machine will try to get back to Point C' in order to keep equilibrium. On the half way of this transition, if the machine moves across the stability limit, the machine will overturn.

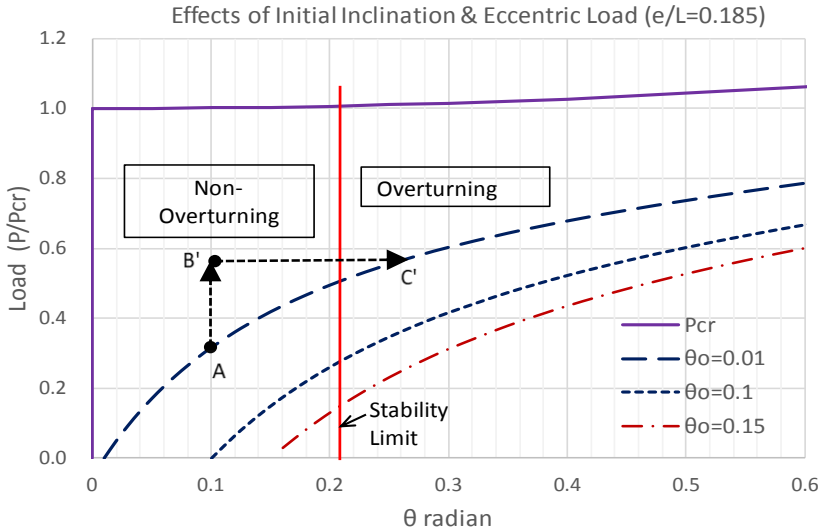


Figure 4. Mechanism of Type of Equilibrium Transition (e/L = 0.185).

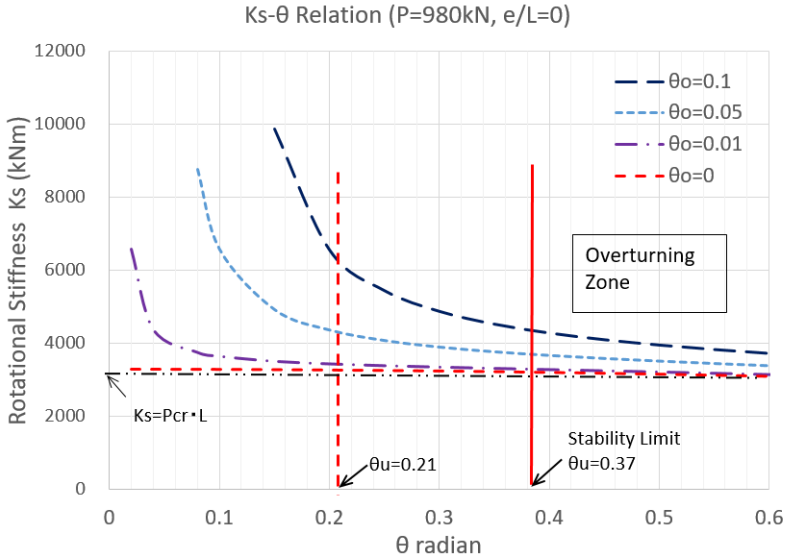


Figure 5. Rotational Stiffness-Displacement Curves.

Likewise, the mechanism of the type of equilibrium transition is explained in Figs. 5 through 7 in the Ks -θ plane, which are calculated for a sample of the pile driving machine with the weight 980kN. In Fig. 5 it can be seen that the effects of *Ks* and θ_0 are remarkable: the smaller the rotational stiffness *Ks*, the larger the displacement θ; and the larger the initial inclination θ_0, the larger the displacement θ. Especially it should be noted that the initial inclination reduces significantly the overturning stability as also seen previously in Fig.2.

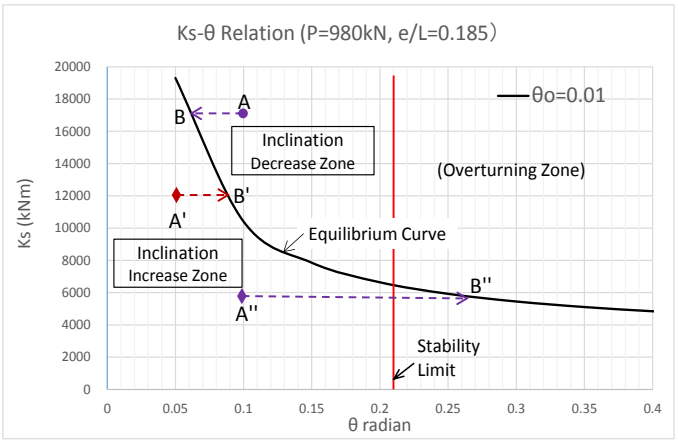
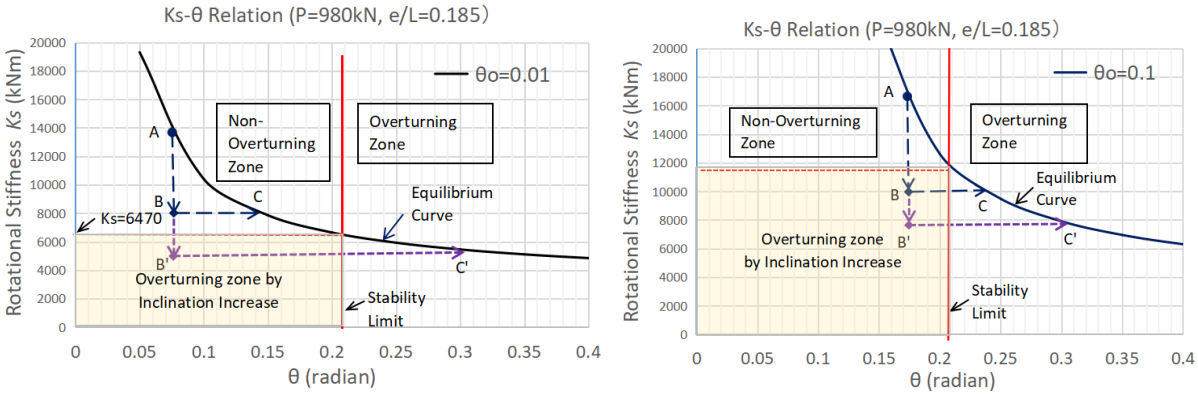


Figure 6. Inclination Increase and Decrease Zones. Zones.

Figure 6 shows an equilibrium curve taken from Fig. 5. The right side to the curve in Fig. 6 is the inclination decrease zone because the righting moment is larger than the overturning moment in this region, thus the displacement at Point A will decrease toward Point B; vice versa on the left side, thus the displacement at Point A' will increase to Point B'. If the machine is located at a softer point at A'', it will move toward Point C'', crossing the stability limit to overturn.



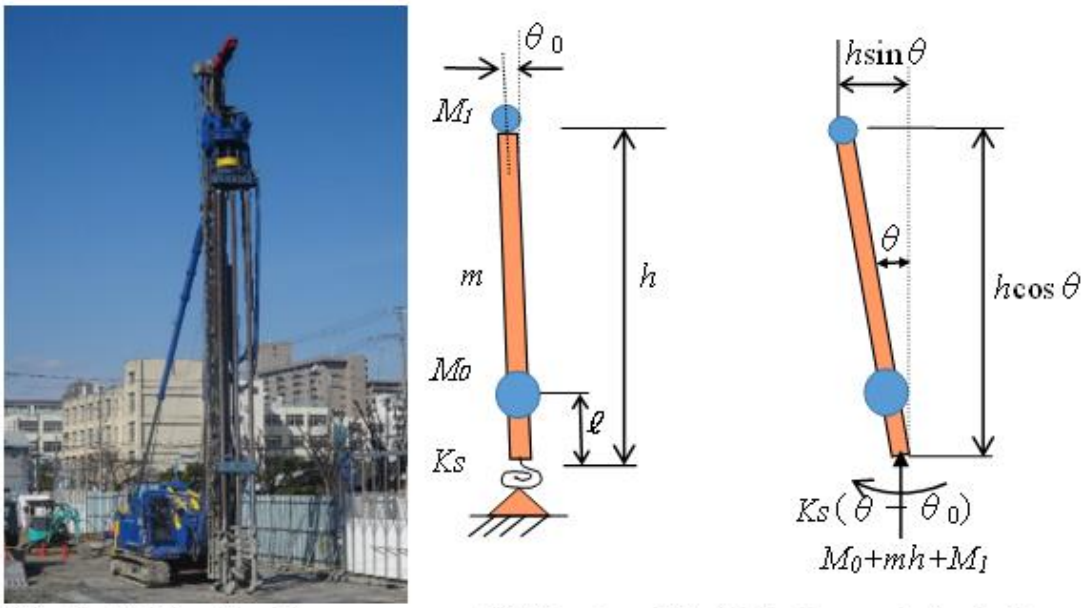
(a) Initial Inclination θ_0=0.01 (b) Initial Inclination θ_0=0.1

Figure 7. Overturning Conditions of Type of Equilibrium Transition.

The intersection of the stability limit and the equilibrium curve in Figure 7 indicates the boundary of the stable and unstable. Therefore, the colored area in Fig. 7 is the overturning zone; when the initial inclination is small as shown in Fig. 7 (a), the overturning zone is small; and vice versa in Fig. 7 (b).

OVERTURNING MECHANISMS BY DYNAMIC ANALYSIS

Structural Model and Equations of Motion



(a) Pile Driving Machine (b) Structural Model for Dynamic Analysis

Figure 8. Pile Driving Machine and Structural Model for Dynamic Analysis.

In the static analysis, the structural model of the pile driving machine is taken as shown in Fig. 1, in which the whole mass is concentrated at the center of gravity, i.e., one-mass structural

system. This is because the static analysis can be dealt with at the first order moment. In the dynamic analysis, however, since the inertia moment (second order moment) is involved, a three-mass system is adopted as shown in Fig. 8. Namely, the whole mass is divided into the three parts to represent the entire pile driving machine: lower machinery part M_0 (kg), auger on top M_1 (kg) and the arm m (kg/m). The former two are a concentrated mass and the last is a distributed mass. It should be noticed that in the dynamic analysis those three are the mass, not the weight in the static analysis. In Fig. 8, ℓ is the distance to the mass M_0, and h is the distance to the mass M_1 which equals to the arm length. Note that the height L in Fig. 1 in the static analysis is the distance to the center of gravity of the whole weight.

In accordance with the structural model in Fig. 8, the equation of motion is derived as follows:

$$I\frac{d^2\theta}{dt^2} + \gamma\frac{d\theta}{dt} - T\sin\theta + K_s(\theta - \theta_0) = 0 \qquad (6)$$

The first term of Eq. (6) is the inertia moment; the second is the attenuating moment; the third is the overturning moment; and the fourth is the righting moment induced by the ground support. Comparing Eq. (6) with Eq. (1) in the static analysis, it can be seen that the first and the second terms are added. The inertia moment I is obtained by the second order moments in Eq. (7).

$$I = \left(M_1 + \frac{1}{3}mh\right)h^2 + M_0\ell^2 \qquad (7)$$

On the other hand, the first order moment of the whole machine weight T is expressed with the acceleration of gravity g =9.8(m/sec^2) as

$$T = \left(M_1 + \frac{1}{2}mh\right)gh + M_0g\ell \qquad (8)$$

Since the second order moment is involved in the dynamic analysis, the effect of the height is larger than the static analysis. The equation of motion Eq. (6) will be solved in the next.

Solutions for Equations of Motion

For simplicity to solve Eq. (6), it is assumed that the coefficient of attenuation γ is zero and the displacement inclination θ is infinitesimal, i.e., $\sin\theta \approx \theta$. Then, Eq. (6) becomes

$$I\frac{d^2\theta}{dt^2} + (K_s - T)\theta - K_s\theta_0 = 0 \qquad (9)$$

In order that the machine is stable, the righting moment has to be larger than the overturning moment, i.e., $Ks > T$. Here, the parameter α is introduced as the ratio of T to Ks.

$$\frac{T}{K_s} = \alpha \ (< 1) \qquad (10)$$

From Eq. (10), it can be seen that the smaller the parameter α, the more stable the structural system.

$$\theta = \theta_0, \quad d\theta/dt = \omega_0 \qquad (11)$$

Applying the following initial conditions at t = 0 for the inclination and the angular velocity of inclination

Then, the differential equation Eq. (9) can be solved as follows:

$$\theta(t) = \frac{\omega_0}{\omega}\sin(\omega t) + (\theta_0 - \theta_c)\cos(\omega t) + \theta_c \qquad (12)$$

in which the angular velocity of inclination ω and the central angle of oscillation θ_c are given by

$$\omega = \sqrt{\frac{K_s - T}{I}}, \qquad \theta_c = \frac{\theta_0}{1-\alpha} \ (> \theta_0) \qquad (13)$$

The central angle of oscillation θ_c in Eq. (13) is the solution for θ of Eq. (9) when the angular acceleration of inclination $d^2\theta/dt^2$=0, and θ(t) oscillates with the center θ_c. From the second equation of Eq. (13) α can be replaced by the equation

$$\alpha = 1 - \frac{\theta_0}{\theta_c} \qquad (14)$$

Equation (14) will be used in the numerical study later.

In Case of ω_0=0

Firstly, let us discuss in this section the case of the initial angular velocity of inclination $\omega_0 = 0$. In this case, the displacement inclination of Eq. (12) becomes

$$\theta(t) = (\theta_0 - \theta_c)\cos(\omega t) + \theta_c \qquad (15)$$

Considering the relation $\theta_c < \theta_0$, the displacement inclination θ (t) will be maximum at cos (ω t) = —1, therefore θ_{max} is

$$\theta_{max} = 2\theta_c - \theta_0 = (1+\alpha)\theta_c \qquad (16)$$

If this maximum θ_{max} is larger than the stability limit $\theta_u = \tan^{-1}(S/2L)$ of Eq. (5), the machine will overturn. Thus, the condition to keep stable is $\theta_{max} < \theta_u$, which will lead to

$$(1+\alpha)\theta_c < \tan^{-1}\left(\frac{S}{2L}\right) \qquad (17)$$

in which S is the footing width in Fig. 2, and L is the height of the center of gravity which can be obtained by the equations

$$L = \frac{(M_1 + \frac{1}{2}mh)h + M_0\ell}{M_1 + mh + M_0} = \frac{T}{P}, \qquad P = (M_1 + mh + M_0)g \qquad (18)$$

By multiplying the gravity acceleration g to each term of the left equation of Eq. (18), the numerator becomes the first order moment of each weight, and the denominator becomes the total weight P as defined by the right one of Eq. (18) which is the same P in Eq. (1) used in the static analysis. Looking at the relation between the static and dynamic analyses in conjunction with Eq. (18), the moment T defined by Eq. (8) can be replaced by $T=PL$. This relation leads to the following Eq. (19).

$$\frac{P}{P_{cr}} = \frac{P}{K_s/L} = \frac{PL}{K_s} = \frac{T}{K_s} = \alpha \qquad (19)$$

.

Equation (19) says that the non-dimensioned load coincides with α which is defined previously by Eq. (10). In the above descriptions, it should be noted that θ in the static analysis corresponds to θ_c in the dynamic analysis; the trigonometric functions in the dynamic analysis are approximated as linear; and the eccentricity e is taken as zero.

In Case of $\omega_0 \neq 0$

This section discusses the case that the initial angular velocity of inclination is not zero when the machine is instigated by wind or subjected to rocking during moving. In this case, the effect of the initial angular velocity on the maximum inclination in Eq. (12) has to be acquired. Combining the two trigonometric functions in Eq. (12) turns out to be

$$\theta(t) = \sqrt{(\theta_0 - \theta_c)^2 + (\omega_0/\omega)^2}\,\sin(\omega t + \delta) + \theta_c, \qquad \delta = \tan^{-1}\left(\frac{\theta_0 - \theta_c}{\omega_0/\omega}\right) \qquad (20)$$

in which the second equation of Eq. (20) is the definition of δ. From Eq. (20), the maximum displacement θ_{max} can be derived as shown below in case of $\sin(\omega t + \delta) = 1$.

$$\theta_{max} = \sqrt{(\theta_0 - \theta_c)^2 + (\omega_0/\omega)^2} + \theta_c \qquad (21)$$

The required condition for the machine to remain stable is $\theta_{max} < \theta_u$, which is

$$\sqrt{(\theta_0 - \theta_c)^2 + (\omega_0/\omega)^2} + \theta_c < \theta_u \qquad (22)$$

Naturally, the condition Eq. (22) with $\omega_0 \neq 0$ is severer than the case Eq. (17) with no initial angular velocity of inclination $\omega_0=0$. Numerical study in this case will be described in Sec. 4.3 (4).

In Case of $\theta > \theta_u$

If the displacement inclination exceeds the stability limit, the machine will overturn. Here, the behavior of the machine after exceeding the stability limit is studied. In this case, the rotational axis is assumed to move onto the edge point of the footing in Fig. 3, therefore the width of the footing S will be involved in the equation of motion. For simplicity, S is replaced by the following Eq. (23).

$$s = S/2 \qquad (23)$$

In this case, the equation of motion Eq. (6) can be expressed by the following simple form.

$$I\frac{d^2\theta}{dt^2} = U(\theta) \qquad (24)$$

in which the moment of inertia I and the overturning moment $U(\theta)$ are defined below instead of Eqs. (7) and (8).

$$I = M_0\left(\ell^2 + s^2\right) + M_1\left(h^2 + s^2\right) + mh\left(\frac{1}{3}h^2 + s^2\right) \qquad (25)$$

$$U(\theta) = \left(M_0 + M_1 + mh\right)g\left(L\sin\theta - s\cos\theta\right) \qquad (26)$$

In the following discussion, the additional inclination φ after exceeding the stability limit θ_u is introduced.

$$\theta = \theta_u + \phi \qquad (27)$$

By assuming the inclination φ is sufficiently small, the linear approximations $\sin\varphi \approx \varphi$ and $\cos\varphi \approx 1$ can be applied, thus the overturning moment becomes

$$U(\phi) = \left(M_0 + M_1 + mh\right)g\left[\left(L\cos\theta_u + s\sin\theta_u\right)\phi + \left(L\sin\theta_u - s\cos\theta_u\right)\right] \qquad (28)$$

The geometrical relations in Fig 3 leads to the following equations.

$$\sin\theta_u = \frac{s}{\sqrt{L^2+s^2}}, \qquad \cos\theta_u = \frac{L}{\sqrt{L^2+s^2}} \tag{29}$$

Using Eq. (29), the constant term in large bracket of Eq. (28) diminishes and Eq. (28) can be replaced by

$$U(\phi) = T\phi \tag{30}$$

in which the constant T is defined as

$$T = \big(M_0 + M_1 + mh\big)g\sqrt{L^2+s^2} \tag{31}$$

According to the above results, Eq. (24) for θ can be replaced by the equation for φ as follows:

$$I\frac{d^2\phi}{dt^2} = T\phi \tag{32}$$

Applying the initial condition in Eq. (33), the solution for φ(t) is given as shown in Eq. (34).

For $t = 0$ $\qquad \phi = 0$ (33)

$$\phi(t) = C\sinh\big(\omega' t\big), \qquad \omega' = \sqrt{T/I} \tag{34}$$

in which C is an arbitrary constant and the angular frequency of vibration ω' is defined by the second equation of Eq. (34). In order to determine C, the initial angular velocity of inclination ω_0 has to be known. For this purpose, taking Eq. (15) into consideration, the following equation will be derived when $\theta = \theta_u$.

$$\cos(\omega t) = \frac{\theta_u - \theta_c}{\theta_0 - \theta_c} \tag{35}$$

At the same time, the angular velocity $d\theta/dt$ can be obtained by Eq. (15) as follows:

$$\frac{d\theta}{dt} = \omega(\theta_c - \theta_0)\sin(\omega t) \tag{36}$$

Eliminating the time t from the above two equations, $d\theta/dt$ can be expressed by

$$\frac{d\theta}{dt} = \omega\sqrt{(2\theta_c - \theta_0 - \theta_u)(\theta_u - \theta_0)} \tag{37}$$

Let the angular velocity Eq. (37) equals to that of the initial condition for φ(t) in Eq. (34), then

$$\text{For } t = 0 \qquad \frac{d\phi}{dt} = \omega\sqrt{(2\theta_c - \theta_0 - \theta_u)(\theta_u - \theta_0)} \tag{38}$$

From Eq. (38), the constant C is determined and the final solution will be

$$\phi(t) = \frac{\omega}{\omega'}\sqrt{(2\theta_c - \theta_0 - \theta_u)(\theta_u - \theta_0)}\,\sinh(\omega' t) \tag{39}$$

From Eq. (39), it can be seen that the inclination after reaching the stability limit will be increasing exponentially for the machine to overturn. It should be noticed that when the footing width s = 0, the moment of inertia I, Eq. (25), and the overturning moment T, Eq. (31), coincide with the corresponding I and T of Eqs. (7) and (8), respectively, in the case of s=0. Numerical study for φ(t) will be described in Section 6.

RESULTS OF DYNAMIC ANALYSIS

Specifications for Case Studies

In order to make numerical studies for the dynamic analysis, specifications of the pile driving machines, of which the structural model is shown in Fig. 8, are determined in Table 1. The machines have the same whole weight P=980kN for each case, which consists of the three parts, as shown in Fig. 8, with the corresponding weight and the length shown in Table 1. Three kinds of the rotational spring stiffness are studied; Ks=4,000kNm, 7,000kNm and 10,000kNm. The center of gravity L in Table 1 is the height from the rotational center at bottom to the gravity center of the whole machine weight which is the same L as in Fig. 1.

Table 1 Specifications of Pile Driving Machine

	L=3.37, θ u=0.37			Center of Gravity: L=6.18m, Stability Limit Angle: θ u=0.21						
	① θ_0=0.01	② θ_0=0.05	③ θ_0=0.1	④ θ_0=0.05	⑤ θ_0=0.02	⑥ θ_0=0.05	⑦ θ_0=0.1	⑧ θ_0=0.02	⑨ θ_0=0.05	⑩ θ_0=0.1
Rotational Stiffness: Ks (kNm)	4000	4000	4000	4000	7000	7000	7000	10000	10000	10000
Whole Weight: P (kN)	980	980	980	980	980	980	980	980	980	980
Lower Part Weight: $M_0 g$ (kN)	850	850	850	800	800	800	800	800	800	800
Distance to M_0: ℓ (m)	2	2	2	2	2	2	2	2	2	2
Leader Weight: $m g$ (kN/m)	5	5	5	10	10	10	10	10	10	10
Length of Leader: h (m)	20	20	20	27	27	27	27	27	27	27
Upper Part Weight: $M_1 g$ (kN)	30	30	30	30	30	30	30	30	30	30
Center of Whole Gravity: L (m)	3.37	3.37	3.37	6.18	6.18	6.18	6.18	6.18	6.18	6.18
Critical Load: Pcr (kN)	1,188	1,188	1,188	647	1,133	1,133	1,133	1,618	1,618	1,618
P/Pcr (= α)	0.825	0.825	0.825	–	0.865	0.865	0.865	0.606	0.606	0.606
Width of Footing: S (m)	2.6	2.6	2.6	2.6	2.6	2.6	2.6	2.6	2.6	2.6
Stability Limit Angle: θ u	0.368	0.368	0.368	0.207	0.207	0.207	0.207	0.207	0.207	0.207

Remark: g=9.8m/sec^2

The stability limit angle is different depending on the footing width S=2.6m (assumed constant) and the center of gravity L, which is obtained from Eq. (5): they are θ_u=0.368radian(21.1deg.) and 0.207radian(11.9deg.) for L=3.37m and 6.18m, respectively.

Numerical Results of Dynamic Analysis

Substituting each term of the specification in Table 1 into the corresponding equations described in Section 3, numerical studies are made and the results are given in Table 2 for 10 cases of ① through ⑩. It should be noted that the units in Table 2 are based on mass, not weight as used in Table 1. The displacement inclinations θ(t) are plotted in Figs. 9, 10 and 11 respectively for each of the three groups of the cases. In this study, the initial angle velocity is taken as ω_0=0 except to study the effect ofω_0 in Sec. 4.3 (4).

Table 2 Results of Dynamic Analysis

Unit Conversions	L=3.37, θ u=0.37			Center of Gravity: L=6.18m, Stability Limit Angle: θ u=0.21						
1N=1kgm/sec^2 1kN=1000kgm/sec^2 1kNm=1000kgm^2/sec^2	① θ_0=0.01	② θ_0=0.05	③ θ_0=0.1	④ θ_0=0.05	⑤ θ_0=0.02	⑥ θ_0=0.05	⑦ θ_0=0.1	⑧ θ_0=0.02	⑨ θ_0=0.05	⑩ θ_0=0.1
Rot. Stiffness Ksx10^3(kgm^2/sec^2)	4000	4000	4000	4000	7000	7000	7000	10000	10000	10000
Lower Part Mass: M_0 x10^3(kg)	86.7	86.7	86.7	81.6	81.6	81.6	81.6	81.6	81.6	81.6
Distance to M_0: ℓ (m)	2	2	2	2	2	2	2	2	2	2
Leader Mass :m x10^3(kg/m)	0.51	0.51	0.51	1.02	1.02	1.02	1.02	1.02	1.02	1.02
Length of Leader: h (m)	20	20	20	27	27	27	27	27	27	27
Upper Part Mass: M_1 x10^3(kg)	3.06	3.06	3.06	3.06	3.06	3.06	3.06	3.06	3.06	3.06
Moment of Inertia: I x10^3(kgm^2)	2,931	2,931	2,931	9,253	9,253	9,253	9,253	9,253	9,253	9,253
Righting Moment: T x10^3(kgm^2/sec^2)	3,299	3,299	3,299	6,053	6,053	6,053	6,053	6,053	6,053	6,053
Initial Inclination : θ_0	0.01	0.05	0.1	0.05	0.02	0.05	0.10	0.02	0.05	0.10
$\theta c = \theta o/(1-T/Ks)$	0.0570	0.285	0.570	−0.0974	0.148	0.369	0.739	0.0507	0.127	0.253
$\alpha = 1-\theta_0/\theta c (= T/Ks)$	0.825	0.825	0.825	1.513	0.865	0.865	0.865	0.605	0.605	0.605
$\omega = \sqrt{(Ks-T)/I}$ (1/sec)	0.489	0.489	0.489	−	0.320	0.320	0.320	0.653	0.653	0.653
Displacement Inclination: $\theta(t)=(\theta_0-\theta c)\cos\omega t+\theta c$	θ(t)=−0.0470cos(0.489t)+0.0570	θ(t)=−0.235cos(0.489t)+0.285	θ(t)=−0.470cos(0.489t)+0.570		θ(t)=−0.128cos(0.320t)+0.148	θ(t)=−0.319cos(0.320t)+0.369	θ(t)=−0.639cos(0.320t)+0.739	θ(t)=−0.0307cos(0.653t)+0.0507	θ(t)=−0.0767cos(0.653t)+0.127	θ(t)=−0.153cos(0.653t)+0.253
Maximum Inc.: ω_0=0 θ max=2θc−θ_0	0.104	0.521	1.04	$T>Ks$ (転倒)	0.276	0.689	1.38	0.081	0.203	0.407
Maximum Inc.: ω_0=0.05 θ max	0.170	0.542	1.052		0.350	0.725	1.397	0.133	0.235	0.425
Maximum Inc.: ω_0=0.1 θ max	0.267	0.597	1.083		0.485	0.816	1.450	0.207	0.298	0.470

Inclination Behaviors by Dynamic Analysis

(1) Ks=4000×10^3(kgm^2/sec^2), L=3.36m (Cases：①, ②, ③ in Table 2)

Since Eq. (15) in the dynamic analysis ignores the attenuating force, it expresses the simple oscillation with a constant amplitude. Using Eq. (15), the displacement inclination behaviors with respect to time are plotted in Figs. 9 through 11.

Figure 9 shows the cases of Ks=4,000 × 10^3(kgm^2/sec^2), θ_u=0.368rad and α =(T/Ks =P/P_{cr})=0.825 and the initial inclination varies as θ_0 =0.01, 0.05, and 0.1 for the cases ①, ②, ③, respectively in Table 2. Note that these analytical conditions are the same as those of Fig. 2 in the static analysis except θ_0 =0.05 instead of 0.02 [9]. In Fig. 9, the displacement inclination curves show one cycle of oscillation for 13 seconds. The figure illustrates that with the center of oscillation θ_c which is defined by Eq. (13), the inclination will oscillate in the range of the

amplitude. It can be seen from the figure that the larger the initial inclination, the larger the displacement inclination.

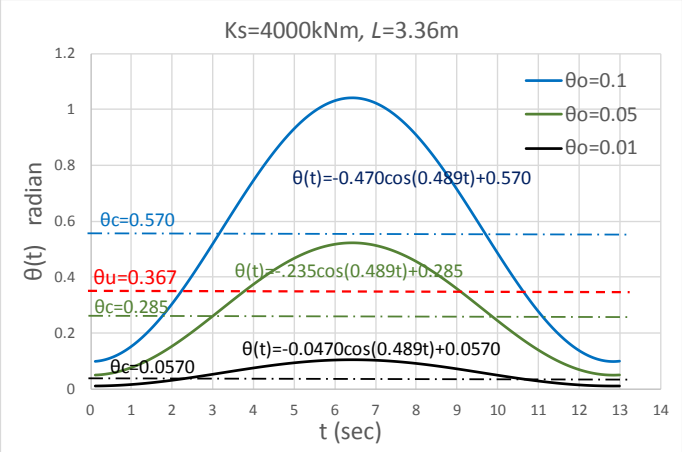


Figure 9. Results of Dynamic Analysis (Cases: ①②③).

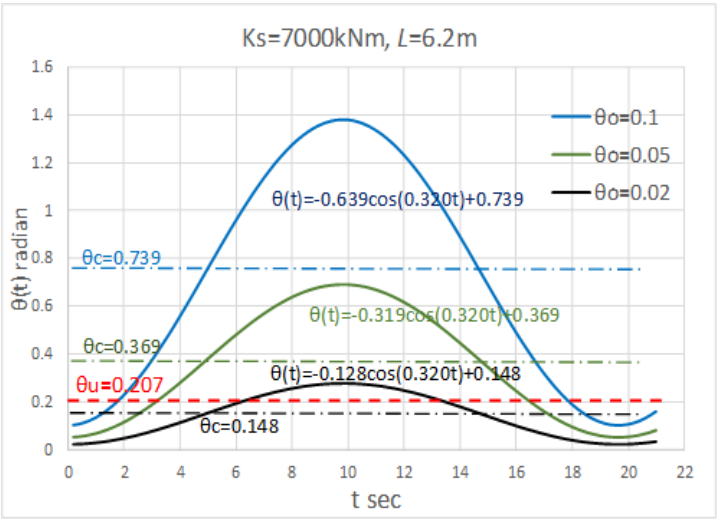


Figure 10. Results of Dynamic Analysis (Cases: ⑤⑥⑦).

It is found from Fig. 9 that except in the case θ_0 =0.01, the maximum inclination θ_{max} exceeds the stability limit θ_u. Then, the rotational stiffness *Ks* which is assumed linear in this study will lose its capability and the machine will overturn. The time to exceed θ_u seems rather short. Once the inclination exceeds θ_u, the displacement inclination will increase exponentially as described later.

(2) Ks=7000×10³(kgm²/sec²), L=3.36m (Cases：⑤，⑥，⑦ in Table 2)

The results of the cases ⑤，⑥ and ⑦ in Table 2 are plotted in Fig. 10, which are for Ks=7,000 ×10³(kgm²/sec²), θ_u=0.207rad. and α=($T/Ks=P/P_{cr}$) =0.865, and the initial inclination varies as

θ_0 =0.02, 0.05 and 0.1, respectively. Compared with Fig. 9, the stability limit is smaller because the center of gravity is higher. Therefore, in all cases the maximum inclination is larger than the stability limit, i.e., $\theta_{max} > \theta_u$, thus the machine will overturn. Also, since the angular velocity of inclination ω is smaller than the cases in Fig. 9, the cycle of oscillation period is longer, i.e., about 20 sec. Therefore, the overturn will occur slowly when the initial inclination is small.

(3) Ks=10000×10³(kgm²/sec²), L=3.36m (Cases：⑧，⑨，⑩ in Table 2)

Figure 11 shows the cases for Ks=10,000×10³(kgm²/sec²), θ_u=0.207rad and α= (T/Ks =P/P_{cr})=0.606, and the initial inclination varies as θ_0=0.02, 0.05 and 0.1. Compared with Fig. 10, since the rotational stiffness is larger, the angular velocity becomes larger and the oscillation period is shorter. The rotational stiffness is directly related to the strength of the ground, which will be a main issue in the future research.

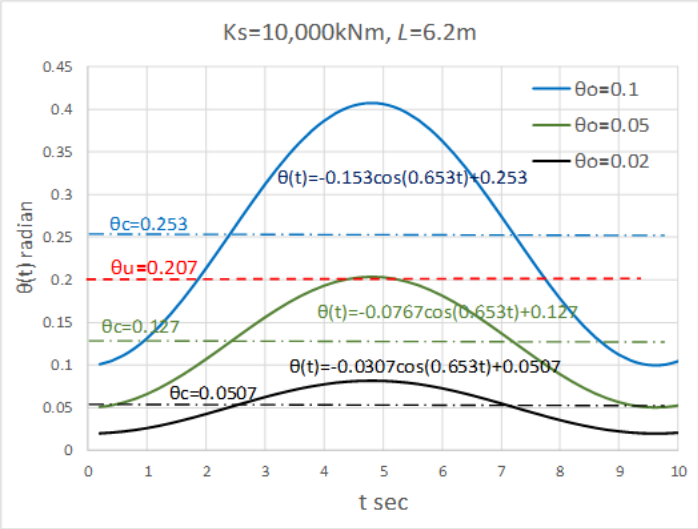


Figure 11. Results of Dynamic Analysis (Cases: ⑧⑨⑩).

(4) **Effect of Initial Angular Velocity**

In the numerical studies so far, the initial angular velocity was assumed zero. Here, based on the equations in Sec. 3.4, the effect of the initial angular velocity of inclination is examined for the case ω_0= 0.05 and 0.1. The results are shown at bottom in Table 2. It is found that the effect on θ_{max} is larger as the initial inclination θ_o is smaller: about 2 times increase for θ_o =0.02 and about 10% for θ_o =0.1. In general, it can be said that the effect is not so large compared to that of the initial inclination. If we consider the attenuating force, the inclination curves in Figs. 9 through 11 will be lowered.

AMPLITUDE OF INCLINATION

Figure 12 shows α-θ_c curves which, because of the relation α=P/P_{cr}, coincide with Fig. 2 in the static analysis. In the figure, also shown are halves of the amplitudes of oscillation ($\theta_0 - \theta_c$) for

the cases ② and ⑨ in Table 2. It should be noted that the abscissa in the dynamic analysis is the oscillation center θ_c. The intersection point of the weight α(=P/P_{cr}) with the curves in Fig. 12 or Fig. 2 expresses the oscillation center for the machine. For example, θ_c=0.285 for the case ② and 0.127 for ⑨ in Table 2 coincide with the intersection points on the curves in Fig.12 at α = 0.825 (red line) and 0.606 (blue line), respectively.

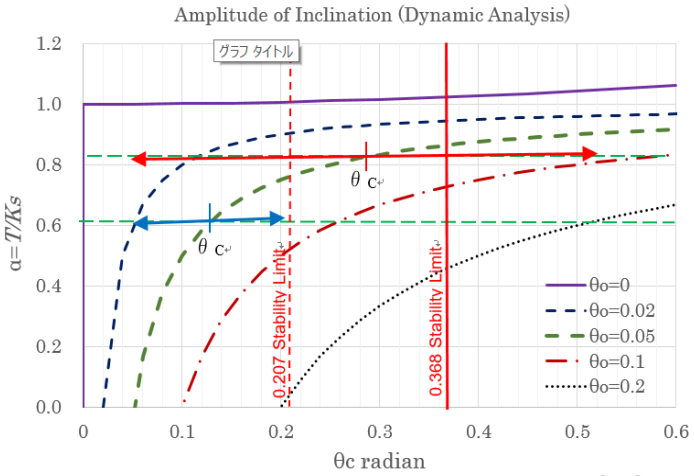


Figure 12. Amplitude of Oscillation (Cases: ②⑨).

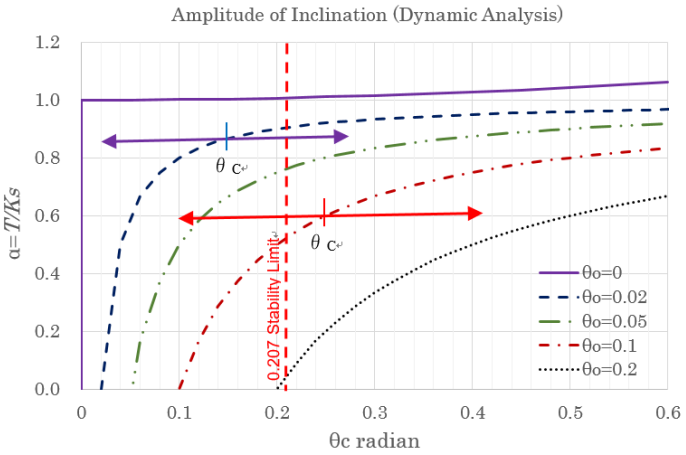


Figure 13 Amplitude of Oscillation (Cases: ⑤⑩).

In the static analysis, the inclination θ (*t)* in Eq. (15) is considered to stay at the equilibrium point θ_c. However, in the dynamic analysis Eq. (15) expresses that the inclination oscillates in the range of amplitude with the center θ_c. This means that the inclination does not stop at the equilibrium θ_c, but continues increasing due to the inertia force. In the case ② (blue line) of Fig. 12, the maximum inclination θ_{max} is less than the stability limit, but in the case ⑨ (red line) θ_{max} is across the stability limit to overturn in the dynamic analysis. Similar results are shown in Fig.

13 for the cases ⑤ (purple line) and ⑩ (red line): the case ⑤ is stable in the static analysis but unstable in the dynamic analysis; the case ⑩ is unstable in both analyses.

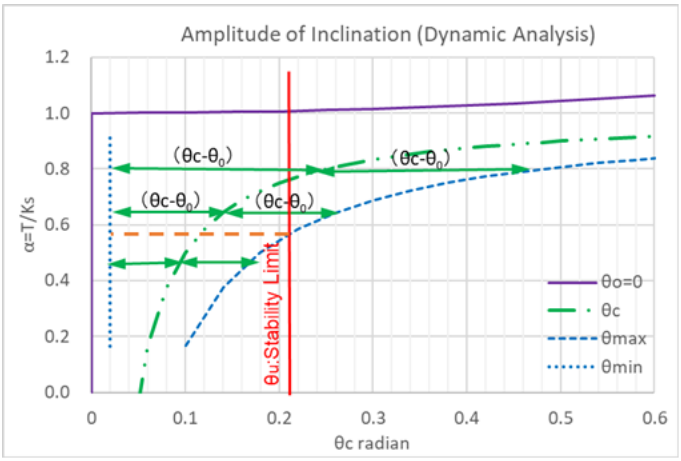


Figure 14. Amplitude of Oscillation (α- *θc* Curves).

Figure 14 shows the oscillation amplitude θ_{max} and θ_{min} with respect to θ_0 =0.05. Since the attenuating force is ignored, the width of the amplitude on the right and the left sides from the center θ_c is the same. It is obvious from Fig. 14 that as $\alpha=P/P_{cr}$ becomes large, the amplitude increases, thus the possibility of overturning increases. At the same time, considering Figs. 12 and 13, the amplitude increases significantly as the initial inclination increases.

Equation (17) in Sec. 3.3 defines the conditions for the machine not to overturn, which can be replaced by the expression $\alpha < \theta_u / \theta_c - 1$. From Fig.14, it is obvious that α (=P/P_{cr}) should not exceed the intersection of the curve θ_{max} and θ_u. On the other hand, it can be understood from the elastic stability (buckling) equation, Eq. (3) $P_{cr}=Ks/L$, that when Ks is small like on the soft ground or the height L is large like high center of gravity, $\alpha=P/P_{cr}$ will be large even if the weight P of the machine remains the same; then, the possibility of overturning will increase.

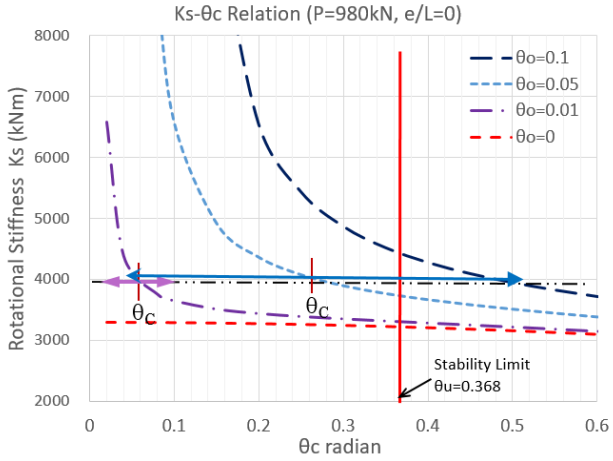


Figure 15. Amplitude of Oscillation (*Ks-θc* Curves).

Figure 15 illustrates the amplitude of oscillation for θ_0 =0.01 and 0.05 in the Ks-θ plane which is previously shown in Fig. 5. Figure 15 describes that the amplitude of the case θ_0 =0.05 is much larger than the case θ_0 =0.01 and exceeds the stability limit. Accordingly, it can be said that the effect of the initial inclination in the dynamic analysis becomes larger compared to the static analysis. Further, the effect of the rotational stiffness *Ks* is significantly large and the anti-overturning capability may be losing exponentially in a certain range. Above all, it should be understood that in the dynamic analysis the displacement inclination will increase by the inertia force and may go over θ_c even θ_u unexpectedly. It should also be noticed that when the attenuating force is considered, the actual maximum inclination θ_{max} will be smaller. Further, the equation of motion Eq. (6) is not valid once the inclination exceeds the stability limit, which will be discussed in the next section.

INCLINATION BEHAVIORS BEYOND STABILITY LIMIT

When the displacement inclination exceeds the stability limit, i.e., $\theta > \theta_u$, theoretical explanation of the dynamic analysis is given in Section 3.5. Using Eq. (39) derived there, the numerical results are shown in Table 3. As can be seen in Table 1 and 2, because of $\theta_{max} < \theta_u$, the cases ①, ④, ⑧ and ⑨ are exempted from this study. According to the results in Table 3, the displacement inclination increases quickly after exceeding the stability limit, and overturns after a couple of seconds.

Table 3 Overturning Behavior after Stability Limit (ϕ(t))

		① θ_0=0.01	② θ_0=0.05	③ θ_0=0.1	④ θ_0=0.05	⑤ θ_0=0.02	⑥ θ_0=0.05	⑦ θ_0=0.1	⑧ θ_0=0.02	⑨ θ_0=0.05	⑩ θ_0=0.1
		全体重心：L=3.37, θu=0.37			全体重心：L=6.18m, θu=0.21						
Ix10^3(kgm^2/sec^2)		3536	3536	3536	6942	6942	6942	6942	6942	6942	6942
I x10^3 (kgm^2)		3100	3100	3100	9439	9439	9439	9439	9439	9439	9439
ω'		1.068	1.068	1.068	0.858	0.858	0.858	0.858	0.858	0.858	0.858
ω/ω'		0.458	0.458	0.458	–	0.373	0.373	0.373	0.762	0.762	0.762
ϕ(t) t (sec)	t=0.1	θ max< θ u	0.011	0.021	θ max< θ u	0.004	0.009	0.011	θ max< θ u	θ max< θ u	0.010
	t=0.5		0.056	0.109		0.019	0.045	0.058			0.049
	t=1		0.129	0.249		0.041	0.099	0.128			0.108
	t=2		0.421	0.812		0.114	0.276	0.355			0.299
	t=3		1.240	2.391		0.275	0.668	0.860			0.725
	t=4		3.612	6.968		0.652	1.583	2.038			1.718
	t=5		10.512	20.279		1.538	3.736	4.808			4.053

Figure 16 shows by the dotted lines the inclination behaviors after exceeding the stability limit for the cases of ② θ_0=0.05 and ③ θ_0=0.1 in Table 3. In the case of ②, since the initial inclination θ_0=0.05 is rather small, i.e., $\theta_c < \theta_u$, the inclination behaviors φ(t) are plotted after θ (t) exceeds θ_u. In this case, the period until overturning is long comparatively. On the other hand, in the case of ③, since the initial inclination θ_0=0.1 is rather large, i.e., $\theta_c > \theta_u$, the machine will overturn in a short tme. As can be seen in Fig. 16, the inclination in both cases increases and reaches the overturning quickly after exceeding the stability limit. This is rational because the machine is in unstable status as shown in Fig. 2 (c) and the righting moment diminishes. It should be

emphasized that in this part of the study the center of overturning rotation is assumed to move from the footing center to the edge of the footing, therefore the mode of the overturning has changed.

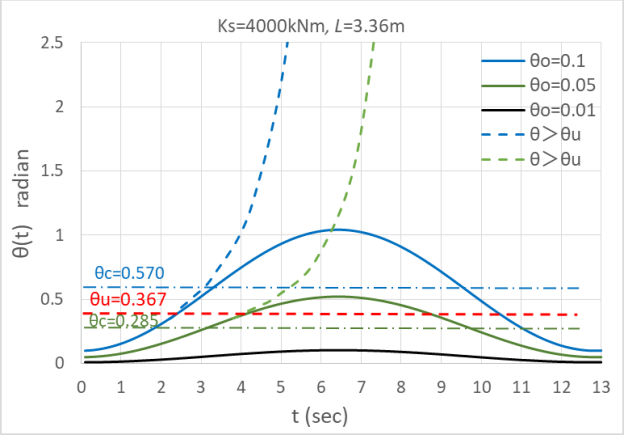


Figure 16. Overturning Behavior Over θ_u (Cases: ②③).

CONCLUSIONS

In the elastic buckling of a long column, a factor of the column length is essential and still important in the elastic-plastic buckling in a short column in which the strength of material becomes more substantial. In this point of view, the overturning problem of the pile driving machine is similar to the short column buckling. The height of the gravity center of the machine corresponds to the length of the column and plays an important role together with the ground support strength and the overturning moment. For instance, the vehicle of a high working platform may overturn only if the arm extends upward and even if the overturning moment remains the same. Also, the overturn might occur when the machine moves to softer ground even if there is no inclination. In this manner, since the machines which have the high gravity center tend to tilt, the effect of the height should be included in prescribing the operation standards.

In the past research, it is pointed out by the authors that in order to avoid overturning accidents the type of the equilibrium transition overturning has to be considered [7-14]. It is shown by the static analysis that there is a possibility of the overturning even if the overturning moment is smaller than the righting moment. In this paper, this type of the overturning mechanism is further studied by applying the dynamic analysis. In the dynamic analysis, the equation of motion is derived and solved to see the overturning behaviors by providing the numerical results for some sample machines. Theory of the dynamic analysis can explain more precisely the possibility of overturning than the static analysis.

After all, in order to avoid the overturning accidents of the heavy machines such as pile driving machines, cranes, jacks and working vehicles with long arms, etc., which frequently occurred recently, the height of the gravity center has to be considered in the safety standards. It is hoped that this paper would contribute to making the safety standards.

References

[1] Nikkei Construction, Special Issue. (2000). Accidents under Construction, Preventing Measures for Recurrence by Learning from Great 70 Accidents, Overturning Accidents of Heavy Machines, Nikkei BP, November. (In Japanese).

[2] Accidents 100, Collection of Examples, (General Inc. Association) Federation of All Japan Foundation Construction Group, http://www.kt.rim.or.jp/~zenkiren/contents/example.html

[3] Crane Related Accidents-Examples of Disaster, (General Inc. Association) Japan Construction Machinery and Construction Association, https://jcmanet.or.jp/bukai-iinkai/kensetsugyou-bukai/saigai-jirei/

[4] Pile Driving Contractors Association (PDCA). (2017). Pile Driving Safety and Environmental Best Management Practices, September.

[5] Pile Driving Contractors Association (PDCA). (2021). Working Platforms Recommended Industry Practices.

[6] Hori T., Tamate S. and Suemasa N. (2010). Measurement of Shakes and Ground Contact Pressure of a Drill Rig by the Self-Propelled Experiments, Journal of Japan Association of Civil Engineering C. May (in Japanese).

[7] Toma, S. (2001). A Study on the Causes of Overturning Accidents of Movable Cranes and Others, 58th Research Report of Hokkaido Branch of Japan Society of Civil Engineers, (in Japanese).

[8] Toma, S. (2016). Causes of Overturning Accidents of Jack and Pile Driving Machine – From a View of Structural Stability –, Abstract Book of Lectures at Annual Meeting of Japan Society of Civil Engineers 2016, Paper No. I-525 (in Japanese).

[9] Toma, S. (2021). Fundamental Cause of Overturning Accidents of Jack and Others, Abstract Book of Lectures at Annual Meeting of Japan Society of Civil Engineers 2021, Paper No. I-52 (in Japanese).

[10] Tome, S. (2021). Causes of Bridge Girder Fall Accidents due to Overturning Jacks, Journal for Japan Society of Safety Engineering, October 60 (5) (in Japanese).

[11] Toma S. (2022). Analysis of Overturning Mechanisms of Pile Driving Machines on Soft Foundation, Kogaku-Kenkyu, Graduate School of Hokkai-Gakuen University, September (in Japanese).

[12] Toma S. and Hoshino J. (2023). A Study of Overturning Stability of Pile Driving Machines, etc. by TDAP Ⅲ, Research Report No. 50, Faculty of Engineering, Hokkai-Gakuen University, January 2023 (in Japanese).

[13] Toma S. and Chen W.F. (2022). Overturning Mechanisms of Jacks, Cranes and Pile Driving Machines, Structural Engineering International (SEI), Taylor & Francis Online, 29 July. DOI:10.1080/10168664.2022.2074339.

[14] Toma S. and Chen W.F. (2022). Some Aspects of Overturning Mechanisms of Pile Driving Machine on Soft Foundation, American Journal of Civil Engineering, pp. 225-232, DOI: 10.11648/j.ajce.20221006.13, December 2022.

[15] Chen, W.F. and Lui, E. M. (1987). Structural Stability, Theory and Implementation, Chapter 1 General Principles, Elsevier.